ChemComm

Fluorographane (C1HxF1-x-d)n: Synthesis and Properties

Journal:	*ChemComm*
Manuscript ID:	CC-COM-11-2014-008844.R1
Article Type:	Communication
Date Submitted by the Author:	26-Jan-2015
Complete List of Authors:	Sofer, Zdenek; Institute of Chemical Technology, Prague, Department of Inorganic Chemistry Simek, Petr; Institute of Chemical Technology Prague, Department of Inorganic Chemistry Mazanek, Vlastimil; Institute of Chemical Technology, Prague, Department of Inorganic Chemistry Sembera, Filip; Institute of Organic Chemistry and Biochemistry AS CR, v.v.i., Janoušek, Zbyněk; Institute of Organic Chemistry and Biochemistry AS CR, v.v.i., Pumera, Martin; Nanyang Technological University, Chemistry and Biological Chemistry

Journal Name

RSCPublishing

COMMUNICATION

Cite this: DOI: 10.1039/x0xx00000x

Fluorographane $(C_1H_xF_{1-x-\delta})_n$: Synthesis and Properties

Received 00th January 2012,
Accepted 00th January 2012

DOI: 10.1039/x0xx00000x

www.rsc.org/

Zdeněk Sofer[a], Petr Šimek[a], Vlastimil Mazánek[a], Filip Šembera[b], Zbyněk Janoušek[b], Martin Pumera[*c]

Fluorographane $(C_1H_xF_{1-x-\delta})n$ was obtained from graphene by hydrogenation *via* Birch reaction with consequent fluorination of the resulting graphane. Fluorographane exhibits fast heterogeneous electron transfer rates and hydrophobicity, which increase with increasing fluorination.

Hydrogenated graphene is a material with many interesting properties.[1] Hydrogenation of graphene introduces a band gap, which can be tuned from 0 to 3.7 eV for graphene and fully hydrogenated graphene (graph*a*ne), respectively.[2] Hydrogenated graphene exhibits fluorescence and paramagnetism,[3] properties that are not seen in graphene.1 In addition, hydrogenated graphenes exhibit fast heterogeneous electron transfer rates.[4] The properties of hydrogenated graphene can be tuned by the level of hydrogenation.[5-9] In similar manner fluorographene $(C_1F_1)_n$ shows large band-gap which is tunable based on level of fluorination.[10] Fluorographene[11] shows fluorescence and enhanced electrochemical properties[12-14] and its 3D analogue, fluorographite found way to electrochemical application decades ago.[15] In order to add additional vectors to tune the properties of hydrogenated graphene, one can consider covalently bonding a simple electronegative element to the graph*a*ne backbone. Since most of the properties of hydrogen are similar to those of halogens, recently performed theoretical studies on fluorinated graph*a*ne showed that the incorporation of fluorine to graph*a*ne would lead to additional opening of the band gap[16] and that such material exhibits a large piezoelectric effect.[17] Fluorination of materials in general is an excellent way to tune their catalytic properties.[18,19] To best of our knowledge, no experimental report on the synthesis and properties of fluorograph*a*ne has been published. Here, we report the synthesis of fluorograph*a*ne via a two-step method, first involving the creation of C-H bonds in a graphene framework with consequent fluorination of the resulting hydrogenated graphene to create fluorograph*a*ne. We report detailed characterization of fluorograph*a*ne via combustible elemental analysis, X-ray photoelectron spectroscopy (XPS), scanning electron microscopy/X-ray energy dispersive spectroscopy, and infrared spectroscopy along with the heterogeneous electron transfer rates at various $(C_1H_xF_{1-x-\delta})_n$ by cyclic voltammetry. We will show that while it is challenging to fluorinate graphite and graphene, which requires the use of high temperatures (~200-400 °C), the hydrogenated graphene (graph*a*ne) is highly reactive and significant fluorination of graph*a*ne proceeds even at atmospheric pressure fluorination with F_2/N_2 mixture for 1 h. Very high content of fluorine in fluorograph*a*ne can be obtained at longer fluorination times and higher pressures.

Synthesis of hydrogenated graphene was performed *via* Birch reduction process. Graphite was oxidized to graphite oxide (GPO) using the permanganate route (Hummers)[20]; GPO was reduced using hydrazine and hydrogenated via Birch method.3 The resulting hydrogenated graphene (graph*a*ne) of composition 45.54 % at. of C, 49.81 % at. of H, 4.40 % at. of O and 0.26% at. of N of summary formula $C_1H_{1.09}$ was then exposed to various fluorination conditions: hydrogenated graphene was exposed to a fluorine/nitrogen gas mixture (20 vol.% F_2) at a pressure of 1 bar for 1 h; 5 bar for 24 h, and 5 bar for 24 h with consequent fluorination at 12 bar for another 24 h. The resulting materials, labeled accordingly as CHF [1h:1bar], CHF [24h:5bar], and CHF [24+24h:5+12bar] were characterized in detail.

We found that significant fluorination occurs at partial pressures of F_2 as low as 0.2 bar for 1 h and that F_2 1 bar for 24 h saturates graph*a*ne so that a consequent increase of pressure and time does not lead to a significant increase in the fluorine content in

graph*a*ne, reaching a F/C ratio of 0.75. We performed a detailed characterization of the fluorine content as well as of the morphology of the resulting fluorograph*a*nes.

According to a combustible elemental analysis, the fluorograph*a*ne materials prepared by this method contained for CHF[1h:1bar]: 50.10% at. of C, 37.21% at. of H, 8.77% at. of F, 3.69% at. of O and 0.22% at. of N; for CHF[24h:5bar]: 50.77% at. of C, 6.50% at. of H, 38.94% at. of F, 2.68% at. of O and 1.11% at. of N; and for CHF[24+24h:5+12bar]: 47.86% at. of C, 6.78% at. of H, 36.30% at. of F, 8.91% at. of O and 1.24% at. of N. This transfers to a summary formula of $C_1H_{0.74}F_{0.17}$, $C_1H_{0.13}F_{0.77}$, and $C_1H_{0.14}F_{0.73}$, respectively. Delta (δ) in $(C_1H_xF_{1-x-\delta})_n$ stands for the remaining elements, mostly O and traces of N, which were introduced during the synthesis. It is obvious from the results that with the increased time and pressure of fluorination, there is a significant increase in the amount of fluorine at the expense of the amount of hydrogen; one can expect substitution reaction occurring during the fluorination of graph*a*ne. It can be also seen that fluorination proceeds at very mild conditions (0.2 bar F_2, 1 h, room temperature) where the F/C ratio is 0.17 and dramatically increases to the saturation point at higher pressures of 1 bar (24 h) to an F/C ratio of ~0.75. Further increase of pressure and time did not lead to higher content of F in graph*a*ne. Schematic of the proposed structure of fluorographane is shown in Scheme S-1 (ESI).

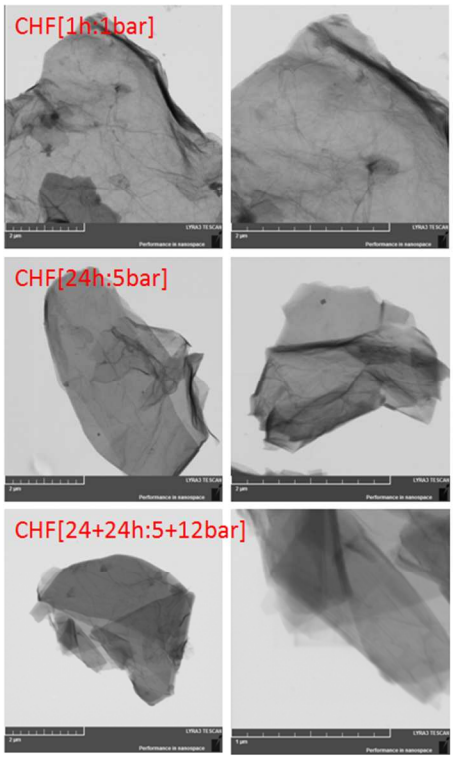

Figure 1. STEM image of fluorograph*a*ne. Left column was obtained at 25 000x and right column was obtained at 50 000x magnification.

Scanning electron microscopy and X-ray energy dispersive spectroscopy (SEM/EDX) were carried out to investigate the morphology as well as the composition of the sample (Figure S-1). SEM images confirmed that fluorinated graph*a*ne sheets are well exfoliated to single-to-few layered structures. SEM/EDX elemental mapping demonstrated that the graph*a*ne sheets are fluorinated homogeneously. EDX spectra showed a F/C ratio of 0.045 in CHF[1h:1bar], 0.62 in CHF[24h:5bar], and 0.75 in CHF[24+24h:5+12bar]. Small differences between the combustible elemental analyses are caused by the surface sensitivity of the SEM/EDX method, morphology of the material, and size of the sample. Note that H content cannot be determined by the EDX method. The presence of single- and few-layered sheets of fluorograph*a*ne is clearly visible in the STEM images (Figure 1).

XPS analysis of the material was performed to reconfirm incorporation of fluorine in fluorograph*a*ne. Wide spectra XPS (Figure 2) shows that fluorograph*a*nes exhibit the following F/C ratios: 0.59 for CHF[1h:1bar], 0.91 for CHF[24h:5bar], and 1.01 for CHF[24+24h:5+12bar]. High resolution spectra of C1s can provide deeper insight into the bond arrangement on the carbon lattice. Figure S-2 shows the fitting of the C1s peaks, demonstrating that with increased time and pressure, there is a shift in the type of fluorinated bonds from C-F to CF_2 and CF_3 (see Table S-1). This can be explained by partial etching of carbon atoms and formation of perfluorinated terminal carbon atoms. Note that XPS cannot provide direct evidence of a C-H bond. We also performed high resolution XPS spectra measurement on F 1s peak (see Figure S-3). The results confirmed the presence of C-F band formation. Slight difference between F/C ratios as determined by various methods originates from different sensitivities of these methods. Combustible analysis takes in account whole sample composition, while XPS is surface sensitive, taking in account only few atomic layers whilst SEM/EDX provides analysis of small portion of the sample.

We performed FTIR measurements of the fluorograph*a*nes, which indicate the presence of both C-H and C-F bonds (Figure S-4). More specifically, for sample CHF[1h:1bar], C-H vibrations are clearly observable at 2845 cm^{-1} and 2915 cm^{-1} with overtones at 1420 cm^{-1}. C-F vibrations are visible at 1040 cm^{-1}. The twinning of C-H bonds indicates the presence of C-H and C-H_2 functional groups. One can observe that the relative intensity of the C-H bond vibrations decreases with increased fluorination pressure/time and that only a weak band at 2950 cm^{-1} originating from the C-H band can be observed in comparison with a very strong C-F vibration band at 1090 cm^{-1} with a weak shoulder at 1200 cm^{-1}. This indicates the formation of CF_2 and CF_3 functional groups under higher pressure / higher temperature fluorine. Detail for C-H bonds is shown on Figure S-5 (ESI). Such observations are consistent with elemental combustible analysis as well as other spectroscopic data.

The Raman spectra of fluorinated graphene are shown on Figure S-6. The Raman spectra of graphene are dominated by two main bands termed as D-band at 1340 cm^{-1} and G-band located at 1565 cm^{-1}. The D/band is associated with the defect in the sp^2 hybridized carbon atoms lattice, while the G-band is associated with the in-plane vibration in the graphene skeletal. In addition we can also observe 2D band at 2670 cm^{-1} and D+G band at 2920 cm^{-1}. The peak observed at 1605 cm^{-1} as a shoulder of G-band us termed as a D' band. The intensity of D' band significantly increase with higher fluorine concentration. Increase of D' band intensity can be associated with the defect induced by graphene etching by high pressure fluorine. This is also documented by AFM images discussed in following paragraph. The I_D/I_G ratio indicates the disorder and defect concentration. The ratio increase with increase of fluorine content from 1.08 for CHF [1h:1bar] to 1.21 for CHF [24h:5bar] and 1.22 for CHF [24+24h:5+12bar] sample. We suggest that the structure of the fluorographane based on the presented analysis is simmilar to graphane with part of the hydrogen atoms exchanged for fluorine atoms, as shown in Figure S-5.

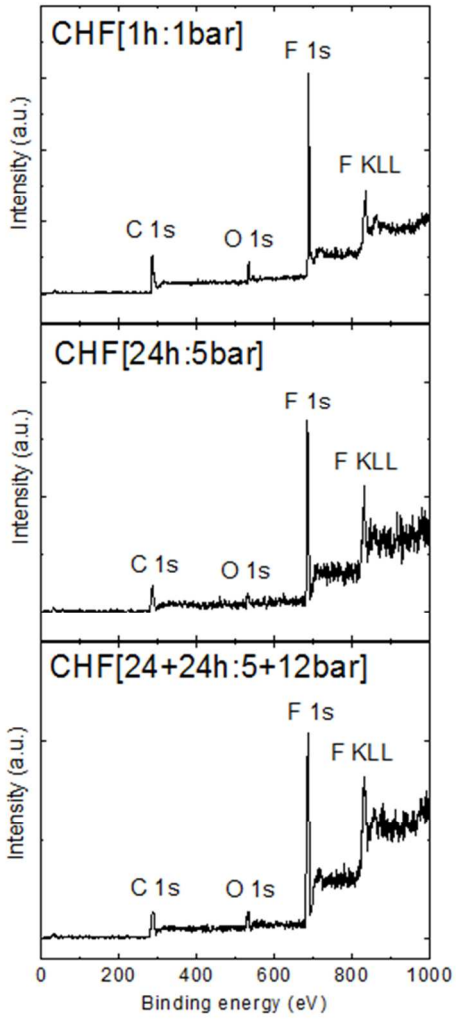

Figure 2. Survey XPS spectra of fluorographane.

The atomic force microscopy (AFM) was used to obtain more information about structure of obtained fluorographane and the influence of increasing of pressure and time used for fluoration. The AFM images are shown in Figure S-7. The thickness of fluorographane slightly increase with higher fluorine concentration form about 0.7-0.8 nm for sample CHF [1h:1bar] to about 0.9-1.0 nm for other two samples with higher fluorine concentration. The fluorographane sheets have flower like structure which indicate intensive etching during fluoration procedure.

Fluorographane have highly hydrophobic properties. These properties can be used for surface modification of various materials. We performed coating of silicon wafer and measured of water contact angle for samples with different fluorine content. The contact able for CHF [1h:1bar] was 109°. The contact angle for CHF [24h:5bar] was 128° and the contact angle for CHF [24+24h:5+12bar]. This demonstrates the possible application of fluorographane for development of protective layers with tailored wetability. The water droplets used for contact angle measurement are shown on Figure S-8. In addition the surface area of fluorgraphane with various degree of fluoration as measured. The surface are of CHF [1h:1bar] is 21.55 $m^2.g^{-1}$, 16.30 $m^2.g^{-1}$ for CHF [24h:5bar] and 16.57 $m^2.g^{-1}$ for CHF [24+24h:5+12bar] sample.

We have studied the electrochemical behavior of fluorographanes. For any electrochemical application, it is important to determine heterogeneous electron transfer of the material. We used ferro/ferricyanide as an electrochemical probe (Fig. 3). Cyclic voltammograms exhibited peak-to-peak (ΔE) separation of 522, 553, and 815 mV for CHF[1h:1bar], CHF[24h:5bar], and CHF[24+24h:5+12bar], respectively. For comparison is also showed peak to peak separation for graphane with ΔE of 663 mV. Heterogeneous electron transfer constant (k^0) was calculated based on DE values using Nicolson's approach.[21] The k^0 found were 1.41×10^{-5}, 9.24×10^{-6}, and 2.64×10^{-7} cm/s for CHF[1h:1bar], CHF[24h:5bar], and CHF[24+24h:5+12bar], respectively. One can see that with increasing fluorine content in fluorographane the k^0 increases. This trend is similar to the trend observed for fluorinated graphites and graphenes, where the HET rates increased with an increased amount of fluorine in the structure.[22,23]

In addition, we wish to demonstrate that with increased fluorination of fluorographane, the hydrophobivity of the material increases, as shown in Figure 4. The contant angle of silicon wafer coated with fluorographane changed from 109° for sample CHF [1h:1bar] to 128°for sample CHF [24h:5bar] and finally 134° for sample CHF [24+24h:5+12bar].Solubility of fluorographane in non-polar solvents is demonstrated in Figure S-7.

In conclusions, we have for the first time successfully prepared fluorographa*n*es with varied ratios of H and F. We used Birch method for preparation of hydrogenated graphene (graph*a*ne) followed with fluorination of the graph*a*ne. This new member of graphene family shows fast heterogeneous electron transfer properties. We expect that fluorogr*a*phane will find variety applications. Changes in the fluorine concentration can be used for development of surface coating with tailored hydrophobic properties.

Acknowledgements:

The project was supported by Czech Science Foundation (Project GACR No. 15-09001S} and by Specific university research (MSMT No. 20/2014). M. P. thanks to Ministry of Education Singapore for Tier 2 grant.

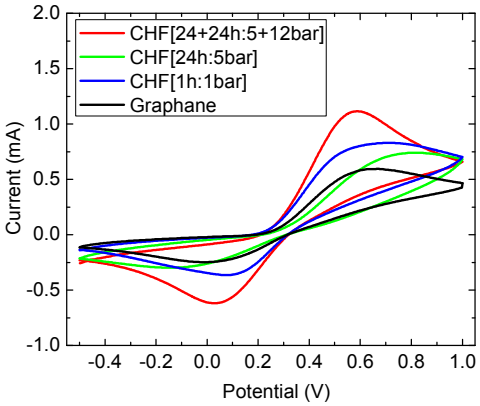

Figure 3. The cyclic voltammetry of fluorographa*n*es and graphane investigated using $[Fe(CN)_6]^{3-/4-}$ redox probe (background electrolyte 50 mM PBS, pH=7.0, 10 mM $K_4[Fe(CN)_6]$, 100 mV/s).

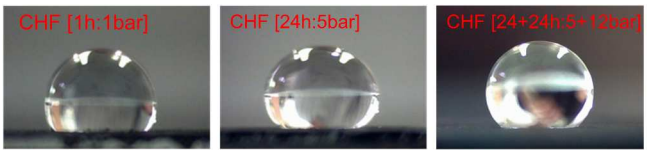

Figure 4. The vetability of fluorographanes decreases with increased fluorine content.

Address

[a] Department of Inorganic Chemistry, Institute of Chemical Technology, Technická 5, 166 28 Prague 6, Czech Republic

[b] Institute of Organic Chemistry and Biochemistry AS CR, v.v.i., Flemingovo náměstí 2, 166 10 Prague 6, Czech Republic

[c] Division of Chemistry & Biological Chemistry, School of Physical and Mathematical Sciences, Nanyang Technological University, Singapore 637371

Notes and references

1 M. Pumera and C. H. Wong, Chem. Soc. Rev., 2013, 42, 5987.
2 J. O. Sofo, A. S. Chaudhari, and G. D. Barber, Phys. Rev. B: Condens. Matter Mater. Phys., 2007, 75, 153401.
3 A. Y. S. Eng, H. L. Poh, F. Šaněk, M. Maryško, S. Matějková, Z. Sofer, and M. Pumera, ACS Nano, 2013, 7, 5930.
4 A. Y. S. Eng, Z. Sofer, P. Simek, J. Kosina, and M. Pumera, Chem. Eur. J. 2013, 19, 15583.
5 R. A. Schafer, J. M. Englert, P. Wehrfritz, W. Bauer, F. Hauke, T. Seyller, and A. Hirsch, Angew. Chem., Int. Ed., 2013, 52, 754.
6 J.D. Jones, C.F. Morris, G.F. Verbeck, J.M. Perez, Applied Surface Science 2013, 264, 853.
7 H. Nejati, M. Dadsetani, Micron, Micron 2014, 67, 30.
8 B.-L. Gao, Q.-Q. Xu, S.-H. Ke, N. Xu,G. Hu, Y. Wang, F. Liang, Y. Tang, S.-J. Xiong, *Phys. Lett. A* 2014, 378, 565.
9 L.B. Drissi, K. Sadki, F. El Yahyaoui, E.H. Saidi, M. Bousmina, O. Fassi-Fehri, *Comp. Materials Science* 2015, 96, 165.
10 R. Zboril, F. Karlicky, A. B. Bourlinos, T. A. Steriotis, A. K. Stubos, V. Georgakilas, K. Safarova, D. Jancik, C. Trapalis, M. Otyepka, Small 2010, 6,
2885.
11 F. Karlický, K. K. R. Datta, M. Otyepka, R. Zbořil, ACS Nano 2013, 7, 6434.
12 R. R. Nair, W. Ren, R. Jalil, I. Riaz, V. G. Kravets, L. Britnell, P. Blake, F.
Schedin, A. S. Mayorov, S. Yuan, M. I. Katsnelson, H.-M. Cheng, W. Strupinski,
L. G. Bulusheva, A. V. Okotrub, I. V. Grigorieva, A. N. Grigorenko,
K. S. Novoselov, A. K. Geim, Small 2010, 6, 2877.
13 H. L. Poh, Z. Sofer, K. Klımova, M. Pumera, J. Mater. Chem. C, 2014, 2, 5198.
14 S. Boopathi, T. N. Narayanan, S. S. Kumar , Nanoscale, 2014, 6, 10140.
15 R. Yazami, Electrochemical Properties of Graphite Fluorides, Metal Fluorides, and Oxide Fluoride-GICs, in Fluorine –Carbon and Fluoride –Carbon
Materials, Chemistry, Physics and Applications (Ed.: T. Nakajima), 1995, Marcel Dekker, New York, pp. 251 –281.
16 R. Paupitz, P. A. S. Autreto, S. B. Legoas, S. G. Srinivasan, A. C. T. van Duin, and D. S. Galvão, Nanotechnol. 2013, 24, 035706.
17 R. A. Brazhe, A. I. Kochaev, and A. A. Sovetkin, Phys. Solid State 2013, 55, 2094.
18 J. C. Yu, J. Yu, W. Ho, Z. Jiang, L. Zhang, Chem. Mater. 2002, 14, 3808-3816.
19 Wingkei Ho, Jimmy C. Yu, and Jiaguo Yu, Langmuir 2005, 21, 3486-3492.
20 W. S. Hummers and R. E. Offeman, J. Am. Chem. Soc. 1958, 80, 1339.
21 Nicholson, R. S. Anal. Chem. 1965, 37, 1351.
22 X. Chia, A. Ambrosi, M. Otyepka, R. Zboril, M. Pumera, Chem Eur J. 2014, 20, 6665.
23 S. Boopathi, T. N. Narayanan, S. S. Kumar, Nanoscale, 2014, 6, 10140.

